



Scientific Journal of Multiple Sclerosis

Research Article

Apoptosis of Moto- and Non-Motoneurons within Moto- And Non-Motoneuron- Enriched Brain Regions in a Mutant Cu, Zn- Superoxide Dismutase Transgenic Mouse Model of Amyotrophic Lateral Sclerosis -

Feng Bao¹ and Danxia Liu^{1,2*}

¹Department of Neurology, University of Texas Medical Branch, Galveston

²Department of Biochemistry & Molecular Biology, University of Texas Medical Branch, Galveston

***Address for Correspondence:** Danxia Liu, Department of Neurology, University of Texas Medical Branch, 301 University Blvd., Rt. 0653, Galveston, TX 77555-0653; Tel: +409-356-6338; E-mail: dliu@utmb.edu

Submitted: 02 February 2018; **Approved:** 17 February 2018; **Published:** 19 February 2018

Cite this article: Bao F, Liu D. Apoptosis of Moto- and Non-Motoneurons within Moto- And Non-Motoneuron-Enriched Brain Regions in a Mutant Cu, Zn-Superoxide Dismutase Transgenic Mouse Model of Amyotrophic Lateral Sclerosis. *Sci J Mult Scler.* 2018; 2(1): 001-009.

Copyright: © 2018 Bao F, et al. This is an open access article distributed under the Creative Commons Attribution License, which permits unrestricted use, distribution, and reproduction in any medium, provided the original work is properly cited.

ABSTRACT

Amyotrophic Lateral Sclerosis (ALS) is a progressive motoneuron degenerative disease; its cause and mechanisms of pathogenesis remain obscure. Apoptosis may be one of the pathways responsible for motoneuron death in ALS. The present study is to further explore the role of apoptosis in ALS. Using a mutant Cu, Zn-superoxide dismutase (mSOD1) transgenic mouse model, we investigated the correlation between SOD1 mutation and neuronal and glial apoptosis in different brain regions. TUNEL-fluorescence staining and ELISA quantification found significantly more DNA fragmentation in mSOD1 mice than in controls. Double staining with TUNEL + an anti-choline acetyltransferase antibody showed many TUNEL-positive motoneurons and glial cells in the spinal cord and brain stem of mSOD1 mice, but not in the controls. Transmission electron microscopy confirmed neuronal and glial apoptosis in the spinal cord, brain stem, and motor cortex by specific morphological features of apoptosis. Double staining with TUNEL + an anti-neuron-specific enolase antibody showed many TUNEL-positive neurons in both the motor and sensory cortices of mSOD1 mice, but not in the controls. Counting the number of TUNEL-positive neurons in the sections from the three mouse groups showed significantly more TUNEL-positive neurons in both the motor and sensory cortices of mSOD1 mice than in the corresponding regions of control mice. There is no significant difference between motor and sensory cortices of mSOD1 mice. These results provide firm *in vivo* evidence that SOD1 mutation induced apoptosis of motoneurons and non-motoneuron cells in motoneuron-enriched brain regions. Therefore, apoptosis is not specific for motoneuron death, but a common pathway causing neuronal and glial degeneration and death in motoneuron-enriched brain regions. SOD1 mutation also induced apoptosis in sensory neurons of sensory cortex. Together, these findings imply that apoptosis might be one of pathways in which the non-neuronal cells and non-motoneuron-enriched brain regions involve in motoneuron death in ALS.

Keywords: Amyotrophic Lateral Sclerosis; Cu, Zn-Superoxide Dismutase Mutation; Neuronal And Glial Apoptosis; Motoneuron Degeneration; Transgenic Mouse Model; Transmission Electron Microscopy

ABBREVIATIONS

Amyotrophic Lateral Sclerosis - ALS; Familial ALS - fALS; Analysis Of Variance - ANOVA; Choline Acetyltransferase - ChAT; Cu, Zn-Superoxide Dismutase - SOD1; Mutant SOD1 - mSOD1; Normal Control - Nc; Hydroxyl Radical - OH; Neuron Specific Enolase - NSE; Peroxynitrite - ONOO⁻; Superoxide Anion - O₂⁻; Phosphate-Buffered Saline - PBS; Reactive Species - RS; Transgenic - Tg; Transmission Electron Microscopy - TEM; Terminal Deoxynucleotidyl Transferase (TdT) Mediated Deoxyuridine Triphosphate-Biotin Nick End Labeling - TUNEL; Enzyme-Linked Immuno-Sorbent Assay - ELISA

INTRODUCTION

Amyotrophic Lateral Sclerosis (ALS) is a progressive degenerative disorder of motoneurons in the spinal cord, brain stem and motor cortex. The disease typically strikes adults, usually causing paralysis and death after five years of symptom onset. A number of mechanisms have been proposed for the pathogenesis of ALS, including genetic factors, oxidative stress, abnormal protein modifications, protein misfolding and aggregation, misregulation of RNA transcription, excess excitotoxicity of glutamate, mitochondrial dysfunction, impaired axonal transport, inflammatory cascades, dysfunctional signaling pathways, and apoptotic cell death. Despite extensive research, the mechanisms of ALS pathogenesis remain obscure, and no effective therapy is available [1-5]. Approximately 10% of ALS cases are inherited. The discovery of mutations in the Cu, Zn-superoxide dismutase (SOD1) gene in familial ALS (fALS) patients [6] was the first breakthrough towards identifying the cause of fALS. Based on this discovery, a Transgenic (Tg) mouse model was established by introducing a mutant human SOD1 gene (Gly 93 → Ala, G93A) into the mouse [7]. These Tg mice developed symptoms resembling human ALS. Although over 100 different SOD1 mutations have been identified in fALS families and a number of Tg mouse models with different mutation sites have been developed [8], most of the research addressing ALS pathogenesis and the development of therapeutic strategies has been performed using the G93A mutant SOD1 (mSOD1) Tg model [9-19]. Therefore, the G93A mSOD1 Tg mouse is still a very powerful and popular animal model for studying the pathogenesis of ALS. The hereditary and non-hereditary forms of

the disease are clinically indistinguishable; thus, the final nerve cell destruction is likely the same for both. Information obtained using the mSOD1 mouse model should therefore also be informative to the much larger number of cases of sporadic, non-inherited ALS. In the present study, the most popular G93A mSOD1 Tg mouse model was used and the results compared with those in wild-type SOD1 (SOD1) mouse and normal mouse (Nc) without gene transfection.

Studies using genetically engineered mouse models have indicated that the expression of mutant SOD1 in neurons alone is insufficient to cause degeneration of motoneurons if they are surrounded by a sufficient number of normal non-neuronal cells [8,20-22]. Conversely, wild type/normal- or mSOD1-deleted motoneurons, surrounded by mSOD1-containing non-neuronal cells lead to signs of abnormality. Therefore, the participation of non-neuronal cells such as microglia [23,24], astrocytes [10,25-27] and oligodendrocytes [28] may contribute to the pathogenesis of the ALS disease [15,29]. These findings changed the concept of ALS as solely a motoneuron degeneration disorder to a complex multi systemic and multifactorial syndrome in which motoneuron degeneration is only part of a wider multifaceted disease process. However, opposite report exist: selective insertion of the G93A SOD1 mutant into motoneurons has shown that these cells inevitably undergo degeneration and death, regardless of the status of the surrounding glial cells [30]. Therefore, it is important to further explore the roles of surrounding non-neuronal cells in this motoneuron degenerative disease.

Apoptosis has been suggested to be one of the pathways responsible for motoneuron death. Apoptosis is important in regulating normal development and maintaining tissue homeostasis in the adult. However, too much or too little apoptosis can result in pathological disorders [31,32]. Molecular evidence from animal and cellular models as well as postmortem tissues indicates that apoptosis occurs in motoneuron death in ALS [11-14,33-36]. However, the morphological evidence for apoptosis in ALS remains equivocal and contradictory [9,12,37]. Therefore, the present study is to provide sound *in vivo* evidence of apoptosis in motoneuron and surrounding non-neuronal cells so as to clarify the role of apoptosis in ALS.

To explore the role of apoptosis in ALS, DNA fragmentation was examined as a biochemical marker of apoptosis by fluorescence

staining of Terminal Deoxynucleotidyl Transferase (TdT)-mediated deoxyuridine triphosphate-biotin nick end labeling (TUNEL)-positive nuclei and by enzyme-linked immuno-sorbent assay (ELISA) in the three groups of mice to determine whether mSOD1 mice are more susceptible to DNA fragmentation than controls are. TUNEL-positive neurons (TUNEL + neuron-specific enolase, NSE) and TUNEL-positive motoneurons (TUNEL+ choline acetyltransferase, ChAT) were double-stained in motor cortex, brain stem and spinal cord – the regions that suffer the most from motoneuron degeneration in ALS – and also in the sensory cortex in the three groups of mice, to explore apoptosis in neurons and motoneurons in different regions of the brain and spinal cord. Neuronal and glial apoptosis was confirmed by their characteristic morphological features among the three groups of mice via Transmission Electron Microscopy (TEM). The DNA fragmentation and morphological characterization provide sound evidence for whether SOD1 mutation induces motoneuron apoptosis, whether apoptosis is specifically for motoneuron death, and whether non-neuronal cells also suffer apoptosis in mSOD1 mice. Comparing the number of TUNEL-positive neurons between motor and sensory cortices in the three groups of mice explores whether in the mSOD1 mice motoneurons in the motor cortex are more susceptible to apoptosis than are sensory neurons in the sensory cortex. Together, these molecular and morphological results clarify the equivocal and contradictory of previous reports regarding the involvement of apoptosis in experimental ALS with strong *in vivo* evidence, and exam whether apoptosis is a pathway in which non-neuronal cells involved in motoneuron death in ALS.

MATERIALS AND METHODS

Animal use

The procedures using mice were approved by the University of Texas Medical Branch Animal Care and Use Committee and were in accord with the NIH Guide for the Care and Use of Laboratory Animals. All efforts were made to use no more animals than needed and to minimize their suffering by careful anesthesia.

Three groups of male mice purchased from the Jackson Laboratory (Bar Harbor, ME, USA) were used: mSOD1 mice transfected with the mutant (G93A) SOD1 gene from humans with fALS - B6SJL-TgN (SOD1-G93A)1Gur; SOD1 mice transfected with the normal human SOD1 gene - B6SJL-TgN (SOD1) 2Gur; and Nc mice - normal control mice (B6SJL-F1) without gene transfection. As reported in our previous publication [38], we found no difference for our measurements when using the littermates of mSOD1 mice, the littermates of SOD1 mice and the normal mice (B6SJL-F1) as controls. Therefore, the B6SJL-F1 normal control mice are a valid control for mSOD1 mice. Based on our previous publications, 3 - 5 data from each group of mice were sufficient for statistical analysis of significant difference [38,39]. In the present study, 4 mSOD1, 4 SOD1, and 6 Nc mice were used for double staining of TUNEL-positive neurons and motoneurons in brain and spinal cord sections. Four additional mice for each group were used for ELISA quantification of DNA fragmentation in brain tissues. The mSOD1 mice died by 4 - 5 months; therefore, 3-month \pm 1 week old mSOD1 mice and age-matched SOD1 and Nc mice were used while paralysis was developing in the mutant strains. The mice were delivered to our housing facility on different dates based on their birthdays, so the surgical operation for tissues harvesting were also performed on different dates to insure all tissues were obtained from each mouse at the age of 3-month \pm 1 week, so that the results are comparable.

Tissue preparation and processing for staining

In all case the mouse was anesthetized with 3% halothane and maintained with 0.5–1% halothane in an oxygen (3 L/min) and air mixture (1:1) until the completion of surgery. After a craniotomy and a laminectomy were performed at vertebrae T 10 - L5, the brain and spinal cord were frozen *in situ* with liquid nitrogen, which also sacrificed the animal. The tissue was then removed and stored at -80°C. Before staining, the frozen brain and spinal cord were fixed in 4% (w/v) paraformaldehyde in 0.01M phosphate-buffered saline (PBS, pH 7.2-7.4) for 24 hours at 4°C, then in 20% sucrose in 0.01M PBS overnight at 4°C. The brain was then cut coronally at the bregma and frozen in liquid nitrogen. Coronal sections of 25 μ m thickness were cut in rostral and caudal directions on a cryostat (IMEB CUT 4500, Leica, Microsystems, Bensheim, Germany). The spinal cords were processed similarly. All sections were collected and kept in 15% sucrose and 0.1% sodium azide in PBS at 4°C until use. Sections selected from the frontal cortex (motor cortex), temporal cortex (sensory cortex), brain stem (medulla oblongata containing hypoglossal nerve nucleus), and spinal cord were processed by free-floating staining as we previously described [39].

Characterization of apoptosis by DNA fragmentation

Apoptosis was characterized by assessing fragmented DNA as a marker of apoptosis, and by morphological identification of specific apoptotic features using TEM.

TUNEL-fluorescence staining of fragmented DNA: To characterize specific DNA fragmentation, TUNEL staining was performed using an ApopTag Fluorescein Direct in Situ Apoptosis Detection Kit (Intergen Company, Purchase, NY, USA) following the manufacture's instruction. Briefly, the floating brain sections were fixed in 1% paraformaldehyde in PBS for 1h and in pre-cooled ethanol: acetic acid (2:1) for 5 min at -20°C. The fixed sections were then immersed in equilibration buffer for 10 min, incubated with TUNEL reagent in a humidified chamber at 37°C for 1 hour, and then incubated in the stop/wash buffer at room temperature for 10 min to stop the reaction. The floating sections were then mounted on slides, coverslipped with PBS/glycerol and stored at 4°C. The fluorescence-stained sections were observed under a Nikon epifluorescence microscope with FITC optics (excitation: BP 450 - 490) to observe TUNEL-positive cells.

TUNEL and immunohistochemical double staining of fragmented DNA in neurons and motoneurons: After fixation and quenching of the endogenous peroxidase in the floating sections in 3.0% hydrogen peroxide in PBS for 5 min at room temperature, TUNEL staining was performed using the ApopTag in Situ Apoptosis Detection Kit (Intergen Company, Purchase, NY, USA) and the reaction stopped as described above. The sections were then washed with three changes of PBS for 1 min each and incubated in anti-digoxigenin peroxidase conjugate for 30 min. After washing in PBS, the sections were visualized with 0.05% diaminobenzidine in staining buffer (0.05% M PBS, pH 7.6). Control sections were treated similarly, but water or equilibration buffer was substituted for the volume of TdT enzyme reagent. To identify TUNEL-positive neurons, the TUNEL-stained brain sections were double-stained with a monoclonal anti-NSE antibody (DAKO, Carpinteria, CA, USA) to identify neurons in motor and sensory cortices. To identify TUNEL-positive motoneurons, the TUNEL-stained sections in the spinal cord and the hypoglossal nerve nucleus were double-stained with a polyclonal antibody directed against ChAT (Abcam, Cambridge, UK).

After TUNEL staining, the sections were washed in three changes of PBS for 5 min each, blocked with 5% goat serum, and incubated with an antibody to ChAT (1:200) or NSE (1:100). After washing in PBS, the sections were incubated with biotinylated goat anti-rabbit-IgG or goat anti-mouse-IgG (1:200, Sigma, St. Louis, MO, USA), then with a solution of an avidin-biotin-horseradish peroxidase complex (1:200, Vector Laboratories, Inc., Burlingame, CA). The sections were then visualized with a SG Substrate Kit (Vector Laboratories, Inc., Burlingame, CA), washed in water, dehydrated, cleaned and coverslipped with Permount.

TEM Characterization of apoptosis by morphological feature

Neuronal apoptosis was confirmed by its specific morphological characteristics using our previously published TEM procedure [40-42]. At 3 months, the mice were anesthetized and sacrificed by transcardial perfusion-fixation with a solution consisting of 4% paraformaldehyde and 2.0% glutaraldehyde in 0.1 M cacodylate buffer (pH 7.2). The frontal cortices, brain stems, and spinal cords (T1-T5) of the mice were removed following a craniotomy and a laminectomy and kept in the same fixative overnight at 4°C. After washing with cacodylate buffer, tissue blocks (0.1×0.1×0.1 mm) were taken from the frontal cortex (layer III-V), brain stem (containing the hypoglossal nerve nucleus) and spinal cord (ventral horn, Rexed layer VIII) under an anatomical microscope and further fixed in 4% osmium tetroxide in 0.1 M cacodylate buffer for 1 hour under a fume hood. The blocks were stained overnight with 2% uranyl acetate at 4°C; the tissue blocks were then dehydrated and embedded in epoxy resin. The semi-thin (1 μm) sections were stained with 1% toluidine blue to locate apoptotic neurons; sections containing apoptotic neurons were cut into ultra-thin sections with an ultramicrotome (Reichert Ultra-cut S; Reichert, Depew, NY, USA), observed by TEM at a magnification of X14,300-42,625 (Phillips CM-100; Philips, Amsterdam, The Netherlands), and photographed.

Quantitative analysis of DNA fragmentation

DNA fragmentation in different brain regions was quantified by counting the double-stained TUNEL-positive neurons. DNA fragmentation in brain tissues was quantified by ELISA.

Quantification by counting TUNEL-positive neurons: For quantitative evaluation of the differences between the motor cortex and sensory cortex in terms of neuronal apoptosis, the TUNEL-positive neurons in motor and sensory cortices were counted within an area of 700 x 400 μm² in layer II-VI of the cerebral cortex under a microscope with a 10x field (Olympus BX40), or 40x for confirmation. Three sequential sections in each animal were counted (3x each) and the counts averaged.

ELISA quantification of DNA fragmentation: After a craniotomy, the mouse brain was frozen *in situ* with liquid nitrogen to avoid oxidative damage during cutting of the tissue; this also sacrificed the animal. The brain was then removed and stored at -80°C for analysis. The frozen brain was homogenized in lysis buffer containing 8 M urea, 0.24 M sodium phosphate, 1% sodium dodecyl sulfate and 10 mM EDTA, pH 6.8, using a 20:1 solution to tissue ratio (v:w). The homogenates were extracted with an equal volume of phenol-chloroform-isoamyl alcohol (25:24:1) saturated with the homogenization buffer. The resulting emulsion was separated into two phases by centrifugation at 4,500 g for 3 min. The aqueous phase above the organic phase was removed for DNA analysis as reported

originally by Beland and coworkers [43] and slightly modified by us [44]. Aliquots (10 μL) of each sample were used to quantitate the nucleosome-associated apoptotic DNA fragments by ELISA using a commercial cell death detection kit (Roche Boehringer Mannheim, Indianapolis, IN, USA) that detects histone-associated DNA fragments enriched in the cytoplasm of a dying cell. The analysis was performed in duplicate according to the manufacturer's instructions.

Statistical analysis

An unpaired *t*-test was used for comparing the difference in DNA fragmentation between mSOD1 mice and each control measured by ELISA in brain tissues. One-way ANOVA followed by the Turkey test was used for statistical analysis of TUNEL-positive neurons in the motor and sensory cortices of the three groups of mice. All data are presented as mean ± SD.

RESULTS AND DISCUSSION

SOD1 mutation significantly increased DNA fragmentation

DNA fragmentation has frequently been used as an indicator of apoptosis. In this study, DNA fragmentation was characterized as a marker of apoptosis by fluorescence staining of TUNEL-positive nuclei as described in the Materials and Methods. The upper panel of figure 1 shows the typical TUNEL-fluorescence-stained nuclei in the frontal cortices of an Nc mouse (A) and an mSOD1 mouse (B) selected from the sections of 4 mSOD1 and 4 Nc mice. Very few TUNEL-positive nuclei were seen in the control section (A). Many TUNEL-positive nuclei were found in the section from mSOD1 mice (B), especially in layer V. This indicated that SOD1 mutation increased the number of TUNEL-positive cells.

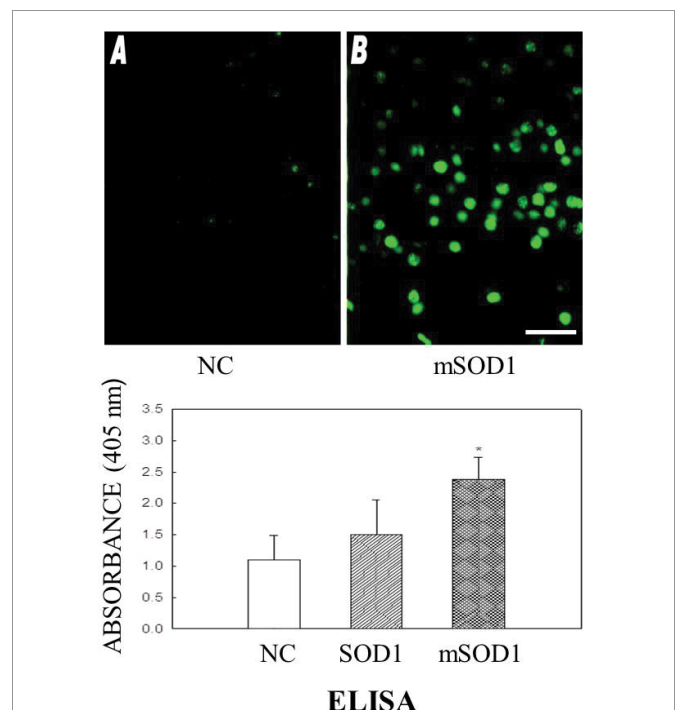


Figure 1: Characterization and quantification of DNA fragmentation: Upper panel, photographs of the representative sections of TUNEL-fluorescence stained mouse frontal cortices: (A) from an Nc mouse; (B) from an mSOD1 mouse. The SOD1 mutation apparently increased the number of TUNEL-positive nuclei. Lower panel, ELISA quantification of DNA fragmentation in brain tissues of three groups of mice. Significantly more DNA fragmentation was found in mSOD1 mice than in SOD1 or Nc mice. Scale bar = 100 μm.

The DNA fragmentation was also quantified by *ELISA* after removal of the brain tissues from the three groups of mice as described in the Materials and Methods ($n = 4$ for each group) and shown in the lower panel of figure 1. The average absorbance (mean \pm SD) was 1.10 ± 0.38 in normal control mice, 1.50 ± 0.55 in normal SOD1-overexpressing mice, and 2.39 ± 0.35 in mutant SOD1 mice. Unpaired *t*-tests demonstrated that there was significantly more DNA fragmentation in mSOD1 mice than in SOD1 ($p = 0.03$) and Nc ($p = 0.002$) mice, with no significant difference between the two control groups ($p = 0.2$). This result demonstrated that SOD1 mutation induced apoptotic-like DNA fragmentation.

SOD1 mutation induced DNA fragmentation in motoneurons

Since ALS is a motoneuron degenerative disorder, to determine whether apoptosis is a pathway for motoneuron death in ALS, motoneuron apoptosis was specifically assessed by double staining with TUNEL and ChAT antibody in the brain stem and spinal cord sections, as described in the Materials and Methods. The motoneurons in the hypoglossal nerve nuclei of the brain stem and the ventral horn of the spinal cord were observed from Nc, SOD1 and mSOD1 mice ($n = 4$ for each group). Figure 2 shows selected typical TUNEL + ChAT double stained sections. Almost no apoptotic motoneurons were observed in the hypoglossal nerve nuclei of the brain stem (Figure 2-left) and the ventral horn of the spinal cord (Figure 2-right) from Nc (A and A' in the left, and A - A'' in the right) and SOD1 (B and B' in the left, and B - B'' in the right) mice. However, many TUNEL + ChAT-positive motoneurons were observed in the sections from mSOD1 mice, both in the hypoglossal nerve nuclei of the brain stem (C and C' in Figure 2-left) and the ventral gray matter of the spinal cords (C - C'' in Figure 2-right). The solid arrowheads in C' (Figure 2-left) and C'' (Figure 2-right) indicate typical TUNEL-positive motoneurons. The fact that many TUNEL + ChAT-positive motoneurons observed in the sections from mSOD1 mice in both regions, but almost no apoptotic motoneurons observed in the corresponding areas in the SOD1 and Nc mice demonstrated that SOD1 mutation induced apoptosis-like DNA fragmentation in motoneurons.

It was noticed that many deeply stained TUNEL-positive nuclei appeared in the sections from mSOD1 mice (C' in the left and C'' in the right of Figure 2), as indicated by hollow arrowheads as examples. This possibly represents apoptosis of other neurons and glial cells.

TEM confirmation of mSOD1 induced neuronal and glial apoptosis

Since DNA fragmentation is not a specific marker for apoptosis; the most reliable identification is via the morphological features of apoptosis [33,37], so DNA fragmentation must be supported by morphological observation. TEM is a gold-standard approach to characterize apoptosis based on specific ultra-structural morphological changes such as cell surface blebbing, cell shrinkage, apoptotic body formation, nuclear chromatin condensation, cytoplasmic organelle compaction, and nuclear lobation [36,45]. In this study, apoptotic neurons and glial cells were characterized by their specific morphological features via TEM observation in ultra-thin sections of the frontal cortex, brain stem (hypoglossal nerve nucleus) and spinal cord ventral horn of the mSOD1 and Nc mice as shown in figure 3. The neurons in the spinal cord and hypoglossal nerve nucleus of the brain stem from normal mice were morphologically normal, showing a large nucleus (N, pale-stained euchromatin) with abundant rough

endoplasmic reticulum (R, Figure 3A and D). The apoptotic neurons in the spinal cord ventral horn (Figure 3B), hypoglossal nerve nucleus (Figure 3E), and motor cortex (Figure 3H) from mSOD1 mice showed condensed chromatin accumulated in the nucleus and condensed cytoplasm. Apoptotic glial cells were also observed in the sections of the spinal cord (Figure 3C), hypoglossal nerve nucleus (Figure 3F), and motor cortex (Figure 3, G and I) from the mSOD1 mice, characterized by condensed chromatin accumulated in the

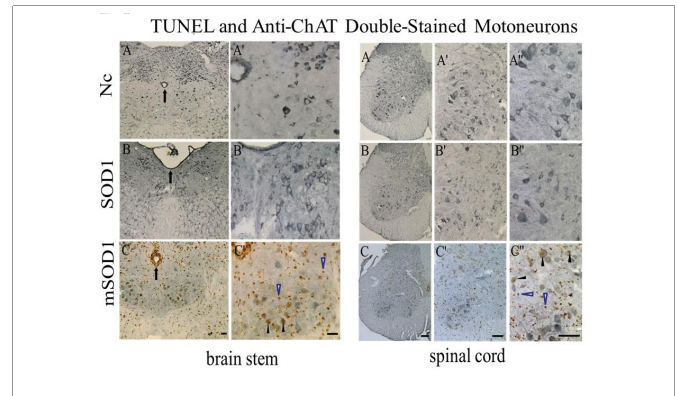


Figure 2: DNA fragmentation in motoneurons: photographs of representative double-stained sections of the brain stem (hypoglossal nerve nuclei, left panel) and ventral horn of spinal cord (right panel). The motoneurons were double-stained with TUNEL and an anti-ChAT antibody: (A) from Nc, (B) from SOD1 and (C) from mSOD1 mice. A', B', and C' are higher magnifications of A, B and C, respectively. A'', B'', and C'' in the right panels are higher magnifications of A', B' and C', respectively. Arrowheads in C' (left panel) and C'' (right panel) of the mSOD1 mouse indicate typical TUNEL-positive motoneurons. Arrows in A, B, and C indicate the central canal. Hollow arrowheads in C' and C'' indicate TUNEL-positive non-motoneurons. Scale bar = 100 μ m.

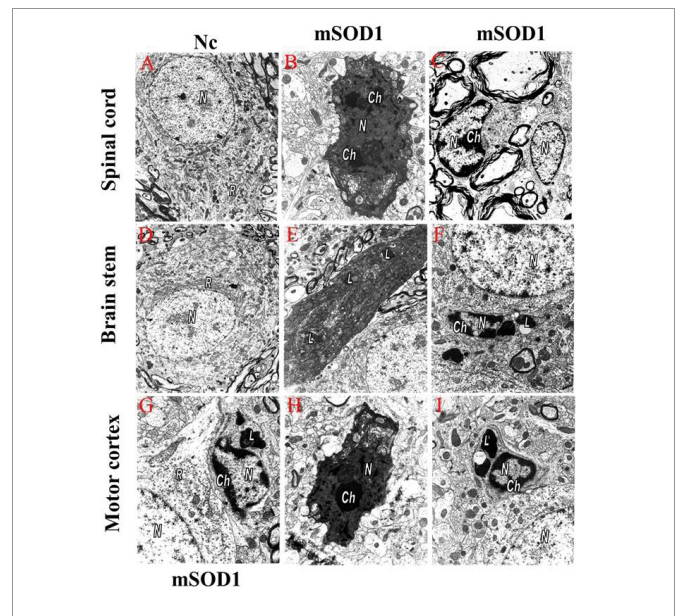


Figure 3: TEM confirmation of neuronal and glial apoptosis: The tissues were fixed and processed for TEM examination as described in the Materials and Methods. A, B, and C from the spinal cord (magnification X10, 725, X24, 475, and X18, 150, respectively) of Nc and mSOD1 mice as indicated. D, E, and F from brain stem (hypoglossal nerve nucleus, magnification X10, 725, X14, 300 and X 24, 475, respectively) of Nc and mSOD1 mice, as indicated. G, H, and I from the motor cortex of mSOD1 mice (magnification X 31, 625, X2 4, 475 and X 24, 475, respectively). Symbols: N, nucleus; R, rough endoplasmic reticulum; Ch, chromatin; L, lipofuscin.



nuclear rim. The apoptotic glial cells shown in Figure 3C are from the white matter of the spinal cord of an mSOD1 mouse, with one cell in an early stage of apoptosis. Figure 3G from the motor cortex of an mSOD1 mouse shows a normal neuron with a large nucleus and abundant rough endoplasmic reticulum and an apoptotic glial cell, characterized by condensed chromatin accumulated in the nuclear rim. These TEM observations clearly show the typical morphology of neuronal (Figure 3, B, E and H) and glial (Figure 3, C, F, G, and I) apoptosis in all three of these regions in mSOD1 mice, but no apoptotic cells were observed in Nc control mice (Figure 3, A and D). Our findings of DNA fragmentation, together with our structural observations by TEM, clearly demonstrated that 1) SOD1 mutation indeed induced apoptotic cell death in the motoneuron-enriched regions; 2) apoptosis is one of the pathways causing cellular degeneration and death in mSOD1 mice, and possibly in fALS; and 3) mSOD1-induced apoptosis is not specific to motoneurons, but is also seen in other neurons and glial cells in the motoneuron-enriched regions. Our finding that not only motoneurons but also glial cells in the motoneuron-enriched regions die via apoptosis supports the idea that neighboring non-motoneuron cells are involved in this motoneuron degenerative disease, as mentioned in the Introduction. Our observation of different stage of glial apoptosis in the white matter of the spinal cord in mSOD1 mice (Figure 3C) indicates that SOD1-induced glial apoptosis is wide spread, not limited to the gray matter of the spinal cord.

It was noticed that a large lipofuscin granule (L) in the cytoplasm appeared near the apoptotic glial cells from the motor cortex (Figure 3, G and I) and brain stem (Figure 3F) in mSOD1 mice. Number of lipofuscin granules were also observed in the apoptotic neuron (Figure 3E). The observation of large lipofuscin granules near the apoptotic glial cells in all apoptotic glia-containing sections from the grey matter of mSOD1 mice (Figure 3, F, G and I), and a number of lipofuscin granules within an apoptotic neuron in a section of an mSOD1 mouse (Figure 3E) suggests that lipofuscin might be involved in the apoptotic cell death processes and play a role in the apoptotic communications between glia and neurons in mSOD1 mice. Although no report can be found regarding this phenomenon, whether the appearance of lipofuscin is related to the onset of cellular apoptosis warrants further study.

SOD1 mutation significantly increased DNA fragmentation in both the motor and sensory cortices

The present study compared neuronal DNA fragmentation between the motor cortex and the sensory cortex. The frontal cortex (motor cortex) and temporal cortex (sensory cortex) of the three mouse groups (n = 4 per group) were double-stained with TUNEL and an anti-NSE antibody as described in the Materials and Methods. Figure 4 illustrates the typical double-stained sections of the motor and sensory cortices selected from the sections in each mouse group. Very few double-stained TUNEL-positive neurons were observed in the sections from Nc and SOD1 mice in both the motor (left panel) and sensory (right panel) cortices. Several double-stained TUNEL-positive neurons were found in both cortices, especially in layer V of the motor cortex and in layer II of the sensory cortex of mSOD1 mice as indicated by solid arrowheads in C". TUNEL-positive nuclei (Non-NSE positive cells) also appeared in both cortices in the sections from mSOD1 mice (C" Figure 4), indicated by hollow arrowheads, possibly representing glial cells. The unexpected finding that TUNEL-positive neurons and possible glial cells not only appeared in the motor cortex but also in the sensory cortex of mSOD1 mice suggested

that apoptosis are not specifically occur in the motoneuron-enriched region and not only limited in the neurons in the later stage of disease.

To quantitatively compare the neuronal apoptosis between motor and sensory regions, TUNEL-positive neurons were counted in the sections from the three groups of mice (n = 4 per group). In the motor cortex, the average number of TUNEL-positive neurons was 0.75 ± 0.95 in Nc mice, 1.67 ± 1.86 in SOD1 mice, and 19.10 ± 6.83 in mSOD1 mice. Statistical analysis by one-way ANOVA followed by the Tukey test indicated that SOD1 mutation induced significantly more TUNEL-positive neurons in the motor cortex of mSOD1 mice than were seen in Nc mice ($p < 0.001$) or SOD1 mice ($p = 0.002$), as shown in the top panel of figure 5. In the sensory cortex, the average number of TUNEL-positive neurons was 0.42 ± 0.50 in Nc mice, 0.78 ± 0.69 in SOD1 mice, and 12.30 ± 6.20 in mSOD1 mice. The SOD1 mutation thus also significantly increased

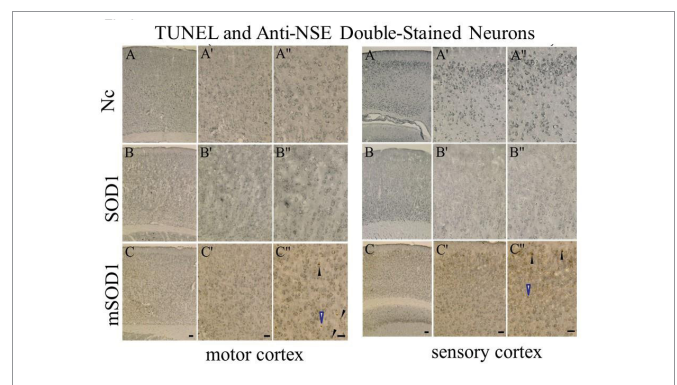


Figure 4: DNA fragmentation in neurons of motor and sensory cortices: Photographs of representative sections from the motor (left panel) and sensory (right panel) cortices, double-stained with TUNEL and an anti-NSE antibody. Section A from Nc, section B from SOD1, and section C from mSOD1 mice. A', A'', B', B'', C', and C'' are higher magnifications of A, B and C, respectively. Solid Arrowheads in C'' indicate TUNEL-positive neurons. Hollow arrowheads in C'' indicate TUNEL-positive non-neuronal cells. Scale bar = 50 μ m.

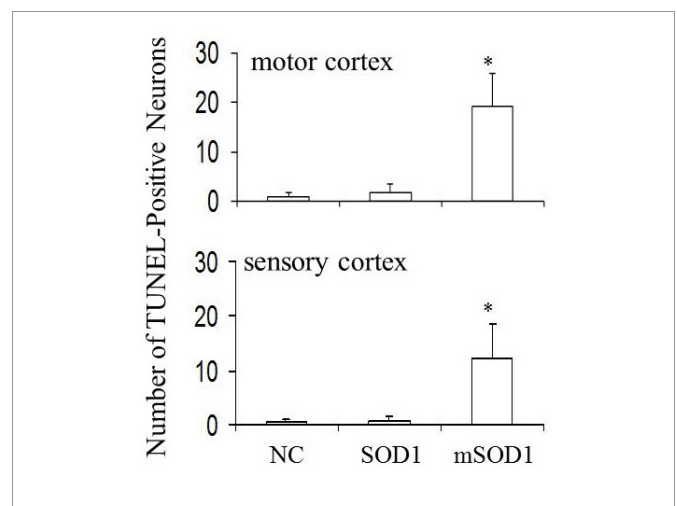


Figure 5: Quantitative comparison of DNA fragmentation between motor and sensory cortices: TUNEL and anti-NSE antibody double-stained TUNEL-positive neurons were counted in layers II-VI of the motor and sensory cortices, as described in the Materials and Methods. The counts were compared among the three groups of mice and statistically analyzed by one-way ANOVA followed by the Tukey test. The number of TUNEL-positive neurons was significantly higher in both the motor and sensory cortices of mSOD1 mice than in Nc and SOD1 mice. There was no significant difference between motor and sensory cortices in the mSOD1 mice.

DNA fragmentation in the sensory cortex compared to Nc mice ($p = 0.006$) and to SOD1 mice ($p = 0.01$) (Figure 5, bottom panel). There were no significant differences between Nc and SOD1 mice in either the motor or sensory cortex. No significant difference was found for the number of TUNEL-positive neurons in the motor cortex vs the sensory cortex ($p = 0.2$) in the mSOD1 mice, although the average number of apoptotic neurons in the motor cortex was higher than in the sensory cortex (19.10 ± 6.83 vs. 12.30 ± 6.20). The finding that SOD1 mutation induced significantly more TUNEL-positive neurons in both the motor and sensory cortices compared to SOD1 and Nc mice (Figure 5) quantitatively demonstrated that apoptosis is not limited to the motoneuron-enriched regions. This is contrary to some earlier reports, such as apoptosis occur in the motor regions (motor cortex and ventral horn of spinal cord) but not in the region unaffected by ALS (somatosensory cortex) [34]; cortical interneuron populations are apparently not affected in mSOD1 mice [13].

The mechanisms by which mSOD1 causes apoptosis are not completely understood. It has been reported that oxidative stress and mitochondrial dysfunction contribute to apoptosis in motoneurons of mSOD1 Tg mice [9,12,34,46-50]. Using the G93A mSOD1 Tg models, our previous studies demonstrate that mutation of SOD1 elevates the *in vivo* levels of Reactive Species (RS), such as hydrogen peroxide (H_2O_2), hydroxyl radical ($\cdot OH$), and nitric oxide. Consequently, the oxidative and nitrative products malondialdehyde (an end product of membrane lipid peroxidation), protein carbonyls (a marker for protein oxidation), 8-hydroxy-2-deoxyguanosine (a marker of DNA oxidation), and protein-bound nitrotyrosine are also significantly elevated in mSOD1 mice compared to SOD1 and Nc mice [38,39]. Elevation of RS and resulting oxidative/nitrative damage in mSOD1 mice have also been reported by many other publications [51,52] as examples. The demonstration of elevation of RS and all markers of oxidation and nitration of protein, DNA and membrane lipids in mSOD1 mice but not in SOD1 and Nc mice strongly supports a correlation between SOD1 mutation and RS generation, with consequent oxidative and nitrative damage. We also demonstrate previously that the generation of $\cdot OH$, H_2O_2 or peroxynitrite ($ONOO^-$) in an uninjured rat spinal cord induces oxidative and nitrative damage [53,54] and necrotic and apoptotic cell death, confirmed by TEM [40-42,55]. These findings demonstrate *in vivo* that RS overproduction indeed induced apoptotic cell death. Together, these results support a possible sequence of: SOD1 mutation \rightarrow elevation of RS \rightarrow oxidative stress to major cellular components \rightarrow apoptotic cell death. We previously report that the number of neurons positively immune-stained for all the markers of protein oxidation and nitration is significantly higher in both the motor and sensory cortices of mSOD1 mice than in controls [39]. The elevated oxidative damage in both the motor and sensory cortices of mSOD1 mice may cause apoptosis in both motor and sensory cortices of mSOD1 mice, further supporting the causal relationship between oxidative stress and apoptotic DNA fragmentation and explaining the reason that apoptosis are not limited in the motoneuron-enriched brain regions. Motoneuron apoptosis has been correlated with RS production and oxidative stress in the mSOD1 model [14,56-58].

The SOD1 mutation, mitochondrial dysfunction, oxidative stress and selective vulnerability of motoneurons are well reviewed by Barber and Shaw [48]. Since SOD1 is ubiquitously expressed and not restricted to motoneurons, it is understandable that motoneurons are not the only cell type affected in ALS. However, motoneurons are unusually large, with a cell body of approximately 50 – 60 μm and an

axon up to 1 m long in humans; therefore, SOD1 is present at higher levels within motoneurons than in other types of cells [59]. The higher level of SOD1 in motoneurons demands a high energy supply from the cellular powerhouse - the mitochondria. In the case of SOD1 mutation, higher levels of mSOD1 and damaged mitochondria cause increased RS production and thereby more severe oxidative stress, and decreased mitochondrial efficiency for supplying energy in the motoneurons of mSOD1 mice. This may lead more motoneurons to go through RS and oxidative stress-induced apoptotic death. Therefore the major consequence of SOD1 mutation is the selective death of motoneuron populations, although other cells also suffer apoptosis in ALS.

In summary, using molecular and morphological characterization, the present study provides strong *in vivo* evidence that SOD1 mutation indeed induces motoneuron apoptosis in the motor cortex, brain stem and ventral horn of the spinal cord; mSOD1-induced apoptosis is not specific to motoneurons, but is also seen in other neurons and glial cells in these motoneuron-enriched regions. This suggests that apoptosis is not specifically for motoneuron death, but a common pathway causing neuronal and glial degeneration and death in mSOD1 mice, and possibly in fALS. It was also found that mSOD1 induces apoptosis in both motor cortex and sensory cortex and there is no significant difference in apoptotic DNA fragmentation in neurons between these regions. This indicates that apoptosis is not specific to neuron death in motoneuron-enriched regions, but also causes sensory neuron death in mSOD1 mice at the later stage of ALS. Our TEM observation that large lipofuscin granules appeared near the apoptotic glial cells in all apoptotic glia-containing sections from the grey matter of mSOD1 mouse and a number of lipofuscin granules were also found within an apoptotic neuron in a section of an mSOD1 mouse. Although the role of lipofuscin has not been reported, we assume that lipofuscin might be involved in the apoptotic cell death processes and play a role in the apoptotic communications between glia and neurons in mSOD1 mice.

ACKNOWLEDGMENTS

This work was supported by a grant from the Amyotrophic Lateral Sclerosis Association to D Liu and also supported by Dr. Liu's MSRDP account from the Department of Neurology, University of Texas Medical Branch. The authors thank Dr. David Konkel for editorial assistance during manuscript preparation.

REFERENCES

- Shaw PJ. Molecular and cellular pathways of neurodegeneration in motor neurone disease. *J Neurol Neurosurg Psychiatry*. 2005; 76: 1046-1057. <https://goo.gl/AhxgTD>
- Pandya RS, Zhu H, Li W, Bowser R, Friedlander RM, Wang X. Therapeutic neuroprotective agents for amyotrophic lateral sclerosis. *Cell Mol Life Sci*. 2013; 70: 4729-4745. <https://goo.gl/ZmY4mN>
- Tan W, Pasinelli P, Trotti D. Role of mitochondria in mutant SOD1 linked amyotrophic lateral sclerosis. *Biochim Biophys Acta*. 2014; 1842: 1295-1301. <https://goo.gl/CWqMKW>
- Sanhueza M, Chai A, Smith C, McCray BA, Simpson TI, Taylor JP, et al. Network analyses reveal novel aspects of ALS pathogenesis. *PLoS Genet*. 2015; 11: 1005107. <https://goo.gl/1qXe8u>
- Tafari F, Ronchi D, Magri F, Comi GP, Corti S. SOD1 misplacing and mitochondrial dysfunction in amyotrophic lateral sclerosis pathogenesis. *Front. Cell Neurosci*. 2015; 9: 336. <https://goo.gl/JFrnHi>
- Rosen DR, Siddique T, Patterson D, Figlewicz DA, Sapp P, Hentati A, et al. Mutations in Cu/Zn superoxide dismutase gene are associated with familial amyotrophic lateral sclerosis. *Nature*. 1993; 362: 59-62. <https://goo.gl/oL62of>

7. Gurney ME, Pu H, Chiu AY, Dal Canto MC, Polchow CY, Alexander DD, et al. Motor neuron degeneration in mice that express a human Cu,Zn superoxide dismutase mutation. *Science*. 1994; 264: 1772-1775. <https://goo.gl/VDA1UA>
8. Gonzalez de Aguilar JL, Echaniz-Laguna A, Fergani A, René F, Meininger V, Loeffler JP, et al. Amyotrophic lateral sclerosis: all roads lead to Rome. *J Neurochem*. 2007; 101: 1153-1160. <https://goo.gl/NM6N4W>
9. Martin LJ, Liu Z, Chen K, Price AC, Pan Y, Swaby JA, et al. Motor Neuron Degeneration in Amyotrophic Lateral Sclerosis Mutant Superoxide Dismutase-1 Transgenic Mice: Mechanisms of Mitochondriopathy and Cell Death. *J Comparative Neurol*. 2007; 500: 20-46. <https://goo.gl/CzeUhx>
10. Cassina P, Cassina A, Pehar M, Castellanos R, Gandelman M, de Leon A, et al. Mitochondrial dysfunction in SOD1G93A-bearing astrocytes promotes motor neuron degeneration: prevention by mitochondrial-targeted antioxidants. *J Neurosci*, 2008; 28: 4115-4122. <https://goo.gl/nKnTmT>
11. Zhang X, Chen S, Li L, Wang Q, Le W. Folic acid protects motor neurons against the increased homocysteine. *Neuropharmacol*. 2008; 54: 1112-1119. DOI: <https://goo.gl/oWsjif>
12. Reyes NA, Fisher JK, Austgen K, VandenBerg S, Huang EJ, Oakes SA. Blocking the mitochondrial apoptotic pathway preserves motor neuron viability and function in a mouse model of amyotrophic lateral sclerosis. *J Clin Invest*. 2010; 120: 3673-3679. <https://goo.gl/fMCjDq>
13. Ozdinler PH, Benn S, Yamamoto TH, Guzel M, Brown RH Jr, Macklis JD. Corticospinal motor neurons and related subcerebral projection neurons undergo early and specific neurodegeneration in hSOD1G93A transgenic ALS mice. *J Neurosci*. 2011; 31: 4166-4177. <https://goo.gl/fwfm8>
14. Xu R, Wua C, Zhang X, Zhanga Q, Yang Y, Yia J, et al. Linking hypoxic and oxidative insults to cell death mechanisms in models of ALS. *Brain Res*. 2011; 1372: 133-144. <https://goo.gl/tchBjN>
15. Lee D-Y, Jeon GS, Shim Y-m, Seong S-Y, Lee K-W, Sung J-J. Modulation of SOD1 subcellular localization by transfection with wild- or mutant-type SOD1 in primary neuron and astrocyte cultures from ALS Mice. *Exp. Neurobiol*. 2015; 24: 226-234. <https://goo.gl/TXix4Y>
16. Jiang HZ, Wang SY, Yin X, Jiang HQ, Wang XD; Wang J. et al. Downregulation of Homer1b/c in SOD1 G93A models of ALS: A novel mechanism of neuroprotective effect of lithium and valproic acid. *Int J Mol Sci*. 2016; 17. <https://goo.gl/jrHppH>
17. Golko-Perez S, Amit T, Youdim MB, Weinreb O. Beneficial effects of multitarget iron chelator on central nervous system and gastrocnemius muscle in SOD1(G93A) transgenic ALS mice. *J Mol Neurosci*. 2016; 59: 504-510. <https://goo.gl/Uw9yha>
18. Zhang Y, Li H, Yang C, Fan DF, Guo DZ, Hu HJ, et al. Treatment with hydrogen-rich saline delays disease progression in a mouse model of amyotrophic lateral sclerosis. *Neurochem Res*. 2016; 41: 770-778. <https://goo.gl/j1FAVf>
19. Zhou QM, Zhang JJ, Li S, Chen S, Le WD. n-Butylidenephthalide treatment prolongs life span and attenuates motor neuron loss in SOD1^{G93A} mouse model of amyotrophic lateral sclerosis. *CNS Neurosci & Therapeutics*. 2017; 23: 375-385. <https://goo.gl/J1Xwff>
20. Pramatarova A, Laganieri J, Roussel J, Brisebois K, Rouleau GA. Neuron-specific expression of mutant superoxide dismutase 1 in transgenic mice does not lead to motor impairment. *J Neurosci*. 2001; 21: 3369-3374. <https://goo.gl/bdKTzR>
21. Lino MM, Schneider C, Caroni P. Accumulation of SOD1 mutants in postnatal motoneurons does not cause motoneuron pathology or motoneuron disease. *J Neurosci*. 2002; 22: 4825-4832. <https://goo.gl/PeUsxn>
22. Clement AM, Nguyen MD, Roberts EA, Garcia ML, Boillée S, Rule M, et al. Wild-type nonneuronal cells extend survival of SOD1 mutant motor neurons in ALS mice. *Science*. 2003; 302: 113-117. <https://goo.gl/F2o5u6>
23. Sargsyan SA, Monk PN, Shaw PJ. Microglia as potential contributors to motor neuron injury in amyotrophic lateral sclerosis. *Glia*. 2005; 51: 241-253.
24. Boillée S, Vande VC, Cleveland DW. ALS: a disease of motor neurons and their nonneuronal neighbors. *Neuron*. 2006; 52: 39-59. <https://goo.gl/uLY9iU>
25. Barbeito LH, Pehar M, Cassina P, Vargas MR, Peluffo H, Viera L, et al. A role for astrocytes in motor neuron loss in amyotrophic lateral sclerosis. *Brain Res Rev*. 2004; 47: 263-274. PMID: 15572176 <https://goo.gl/i8GYgT>
26. Holden C. Astrocytes secrete substances that kills motor neurons in ALS. *Science*. 2007; 316: 353. <https://goo.gl/x18E6M>
27. Cassina P, Pehar M, Vargas MR, Castellanos R, Barbeito AG, Estevez AG, et al. Astrocyte activation by fibroblast growth factor-1 and motor neuron apoptosis: implications for amyotrophic lateral sclerosis. *J Neurochem*. 2005; 93: 38-46. <https://goo.gl/KiQL6J>
28. Ferraiuolo L, Meyer K, Sherwood TW, Vick J, Likhite S, Frakes A, et al. Oligodendrocytes contribute to motor neuron death in ALS via SOD1-dependent mechanism. *Proc Natl Acad Sci USA*. 2016; 113: 6496-6505. <https://goo.gl/grg2jL>
29. Cozzolino M, Rossi S, Mirra A, Carri MT. Mitochondrial dynamism and the pathogenesis of Amyotrophic Lateral Sclerosis. *Front. Cell Neurosci*. 2015; 10: 9-31. <https://goo.gl/jWxdBa>
30. Jaarsma D, Teuling E, Haasdijk ED, De Zeeuw CI, Hoogenraad CC. Neuron-specific expression of mutant superoxide dismutase is sufficient to induce amyotrophic lateral sclerosis in transgenic mice. *J Neurosci*. 2008; 28: 2075-2088. <https://goo.gl/Xi1Jij>
31. Tendi EA, Cunsolo R, Bellia D, Messina RL, Paratore S, Calissano P, et al. Drug target identification for neuronal apoptosis through a genome scale screening. *Curr Med Chem*. 2010; 17: 2906-2920.
32. Miura M. Apoptotic and non-apoptotic caspase functions in neural development. *Neurochem Res*. 2011; 36: 1253-1260. <https://goo.gl/tEoDQc>
33. Sathasivam S, Ince PG, Shaw PJ. Apoptosis in amyotrophic lateral sclerosis: a review of the evidence. *Neuropathol Applied Neurobiol*. 2001; 27: 257-274. <https://goo.gl/ERw4bt>
34. Martin LJ. Mitochondriopathy in Parkinson Disease and Amyotrophic Lateral Sclerosis. *J. Neuropathol. Exp Neurol*. 2006; 65: 1103-1110. <https://goo.gl/ERw4bt>
35. Ilzecka J. Serum caspase-9 levels are increased in patients with amyotrophic lateral sclerosis. *Neurol Sci*. 2012; 33: 825-829. <https://goo.gl/n4jooG>
36. Ghavami S, Shojaei S, Yeganeh B, Ande SR, Jangamreddy JR, Mehrpour M, et al. Autophagy and apoptosis dysfunction in neurodegenerative disorders. *Progress Neurobiol*. 2014; 112: 24-49. <https://goo.gl/jDtDG4>
37. Przedborski S. Programmed Cell Death in Amyotrophic Lateral Sclerosis: a Mechanism of Pathogenic and Therapeutic Importance. *The Neurologist*. 2004; 10: 1-7.
38. Liu D, Wen J, Liu J, Li L. The roles of free radicals in amyotrophic lateral sclerosis: reactive oxygen species and elevated oxidation of protein, DNA, and membrane phospholipids. *Faseb J*. 1999; 13: 2318-2328. <https://goo.gl/qPPsYU>
39. Liu D, Bao F, Wen J, Liu J. Mutation of superoxide dismutase elevates reactive species: comparison of nitration and oxidation of proteins in different brain regions of transgenic mice with amyotrophic lateral sclerosis. *Neuroscience*. 2007; 146: 255-264.
40. Bao F, Liu D. Peroxynitrite generated in the rat spinal cord induces apoptotic cell death and activates caspase-3. *Neuroscience*. 2003; 116: 59-70. <https://goo.gl/xh7b5E>
41. Bao F, Liu D. Hydroxyl radicals generated in the rat spinal cord at the level produced by impact injury induce cell death by necrosis and apoptosis: Protection by a metalloporphyrin. *Neuroscience*. 2004; 126: 285-295. <https://goo.gl/NcBp75>
42. Liu D, Bao F. Hydrogen peroxide administered into the rat spinal cord at the level elevated by contusion spinal cord injury oxidizes proteins, DNA and membrane phospholipids, and induces cell death: Attenuation by a metalloporphyrin. *Neuroscience*. 2015; 285: 81-96. <https://goo.gl/pkzfHF>
43. Beland FA, Dooley KL, Casciano DA. Rapid isolation of carcinogen-bound DNA and RNA by hydroxyapatite chromatography. *J Chromatogr*. 1979; 174: 177-186.
44. Leski ML, Bao F, Wu L, Qian H, Sun D, Liu D. Protein and DNA oxidation in spinal injury: neurofilaments--an oxidation target. *Free Rad Biol Med*. 2001; 30: 613-624. <https://goo.gl/rUAbMo>
45. Wood K A, Youle RJ. Apoptosis and free radicals. *Ann NY Acad Sci*. 1994; 738: 400-407. <https://goo.gl/f4v44s>
46. Cookson MR, Menzies FM, Manning P, Eggett CJ, Figuelewicz DA, McNeil CJ,

- et al. Cu/Zn superoxide dismutase (SOD1) mutations associated with familial amyotrophic lateral sclerosis (ALS) affect cellular free radical release in the presence of oxidative stress. *Amyotroph Lateral Scler Other Motor Neuron Disord.* 2002; 3:75-85. <https://goo.gl/Eun6YB>
47. Muyderman H, Hutson PG, Matusica D, Rogers M-L, Rush RA. The Human G93A-Superoxide Dismutase-1 Mutation, Mitochondrial Glutathione and Apoptotic Cell Death. *Neurochem Res.* 2009; 34: 1847–1856. <https://goo.gl/5hBrrv>
48. Barber SC, Shaw PJ. Oxidative stress in ALS: Key role in motor neuron injury and therapeutic target. *Free Rad Biol Med.* 2010; 48: 629–641. <https://goo.gl/1cKjXu>
49. Drechsel DA, Estévez AG, Barbeito L, Beckman JS. Nitric oxide-mediated oxidative damage and the progressive demise of motor neurons in ALS. *Neurotox. Res.* 2012; 22: 251-264. <https://goo.gl/7RDR4J>
50. Shin JH, Lee YA, Lee JK, Lee YB, Cho W, Im DS, et al. Concurrent blockade of free radical and microsomal prostaglandin E synthase-1-mediated PGE₂ production improves safety and efficacy in a mouse model of amyotrophic lateral sclerosis. *J Neurochem.* 2012; 122: 952-961. <https://goo.gl/wWCHGe>
51. Casoni F, Basso M, Massignan T, Gianazza E, Cheroni C, Salmona M, et al. Protein nitration in a mouse model of familial amyotrophic lateral sclerosis: possible multifunctional role in the pathogenesis. *J Biol Chem.* 2005; 280:16295-16304. <https://goo.gl/1wptdh>
52. Said AM, Hung WY, Zu JS, Hockberger P, Siddique T. Increased reactive oxygen species in familial amyotrophic lateral sclerosis with mutations in SOD1. *J Neurol Sci.* 2000; 176: 88-94. <https://goo.gl/78sPLV>
53. Bao F, DeWitt DS, Prough DS, Liu D. Peroxynitrite generated in the rat spinal cord induces oxidation and nitration of proteins: reduction by Mn (III) tetrakis (4-benzoic acid) porphyrin. *J Neurosci Res.* 2003; 71:220-227. <https://goo.gl/Gu3krZ>
54. Liu D, Bao F, Prough DS, Dewitt DS. Peroxynitrite generated at the level produced by spinal cord injury induces peroxidation of membrane phospholipids in normal rat cord: Reduction by a metalloporphyrin. *J Neurotrauma.* 2005; 22: 1123-1133. <https://goo.gl/LEVBKw>
55. Bao F, Liu D. Peroxynitrite generated in the rat spinal cord induces neuron death and neurological deficits. *Neuroscience.* 2002; 115: 839-849.
56. Cassina P, Peluffo H, Pehar M, Martinez-Palma L, Ressler A, Beckman JS, et al. Peroxynitrite triggers a phenotypic transformation in spinal cord astrocytes that induces motor neuron apoptosis. *J Neurosci Res.* 2002; 1: 21-29. <https://goo.gl/Z24biV>
57. Holasek SS, Wengenack TM, Kandimalla KK, Montano C, Gregor DM, Curran GL, et al. Activation of the stress-activated MAP kinase, p38, but not JNK in cortical motor neurons during early presymptomatic stages of amyotrophic lateral sclerosis in transgenic mice. *Brain Res.* 2005; 1045: 185-198. <https://goo.gl/KoW2gV>
58. Wengenack TM, Holasek SS, Montano CM, Gregor D, Curran GL, Poduslo JF. Activation of programmed cell death markers in ventral horn motor neurons during early presymptomatic stages of amyotrophic lateral sclerosis in a transgenic mouse model. *Brain Res.* 2004; 1027:73-86. <https://goo.gl/4Qk2dh>
59. Pardo CA, Xu Z, Borchelt DR, Price DL, Sisodia SS, Cleveland DW. Superoxide dismutase is an abundant component in cell bodies, dendrites, and axons of motor neurons and in a subset of other neurons. *Proc Natl Acad Sci USA.* 1995; 92: 954–958. <https://goo.gl/4M7ZYp>